Filipin Fluorescence Quenching by Spin-Labeled Probes: Studies in Aqueous Solution and in a Membrane Model System

Miguel Castanho*‡ and Manuel Prieto*
*Centro de Química-Física Molecular, Instituto Superior Técnico, 1096 Lisboa Codex; and ‡Departamento de Química e Bioquímica, Faculdade de Ciências da Universidade de Lisboa, 1700 Lisboa, Portugal

ABSTRACT A detailed photophysical study of the fluorescence quenching (transient and steady state) of the macrolide antibiotic filipin by nitroxide-substituted fatty acids and a cholesterol derivative was carried out, aimed at determining its transverse position in a model system of membranes (multilamellar vesicles of dipalmitoylphosphatidylcholine). Filipin partitions efficiently into membranes (K_p = (5.0 ± 1.0).10^3; 20°C) and it was concluded that the antibiotic is buried in the membrane, away from the lipid-water interface. In addition, information on the organization of the quenchers was also obtained. The 5-nitroxide derivative of the fatty acid is essentially randomly distributed, while the 16-nitroxide is aggregated at concentrations higher than ~5% molar. For the cholesterol compound the results point to a phase separation at concentrations higher than 3% molar (below this limit concentration filipin associates with the derivatized sterol with K_A = 20 M^{-1}, assuming a 1:1 interaction). We propose that this phase separation and the aggregation state of filipin in the aqueous solution may be key processes in the antibiotic mode of action. A systematic and general approach to fluorescence quenching data analysis in complex (e.g., biochemical) systems is also presented.

INTRODUCTION

Filipin, an antibiotic with antifungal properties, belongs to a family of polyenes such as nystatin and amphotericin B, which are characterized by a macrolide structure with an amphipathic nature (Bolard, 1986). We are currently involved in using optical techniques such as fluorescence and ultraviolet-visible absorption (Castanho and Prieto, 1992; Castanho et al., 1992) and light-scattering (Castanho et al., 1994) to obtain information on its supramolecular organization both in aqueous media and associated with model systems of membranes.

Several models have been proposed for the biochemical mode of action of filipin. The presence of sterol in the membrane has long been considered essential (Kinsky et al., 1966), but this idea was recently criticized both in our previously described work and by Milhaud (1992). Regarding the location of filipin in the presence of sterol in the membrane, three situations were described; 1) the antibiotic forms large planar aggregates between the two layers of the membrane (De Kruijff and Demel, 1974); 2) it is adsorbed at the membrane surface (Elias et al., 1979); and 3) it is located at the upper layer of the membrane (Severs and Robenek, 1983). In all cases the structural disorder induced in the membrane would ultimately be responsible for the leakage of cellular components.

It is the primary aim of this work to obtain topological information on filipin in the membrane, i.e., its transverse location. For this purpose we studied its intrinsic fluorescence quenching by fatty acids and sterol labeled with a spin probe. A method was developed for data analysis, which is useful for biochemical systems, providing information on the organization and dynamics of the system.

We also present detailed photophysical data and models on the fluorescence quenching in aqueous solution, as this is essential to understand the complex behavior in the lipidic systems. On the other hand, the derived models for the rationalization of the data in membranes also provides information on both the fatty acids and sterol clustering. Finally, on the basis of our results and the literature, we discuss the main features that influence the antibiotic action of filipin at the membrane level.

MATERIALS AND METHODS

Most of the materials, experimental procedures, and instrumentation both for absorption and steady state and transient fluorescence spectroscopies were recently described (Castanho and Prieto, 1992; Castanho et al., 1992). The single-photon timing technique was used to determine the fluorescence lifetimes and in all cases 10^4 counts were accumulated in the peak channel while background noise was <5 counts. The fluorescence decay data were fitted by a sum of exponential functions and the goodness of the fits was evaluated using the reduced χ^2 parameter and direct inspection of the residuals correlation function. All the data presented in this work correspond to $\chi^2 \leq 1.2$, except for the biexponential decay analyses of filipin incorporated in multilamellar vesicles (MLV) ($\chi^2 \leq 1.5$).

Filipin and L-α-1,2-dipalmitoyl-3-*sn*-glycerophosphatidylcholine (DPPC), 4-hydroxy-Tempo (TEMPOL) and 3-β-doxyl-5 α-cholestane (3NC) were obtained from Sigma Chemical Co. (St. Louis, MO), while 5-doxyl-stearic acid (5NS) and 16-doxyl-stearic acid (16NS) were supplied by Molecular Probes (Eugene, OR). The molecular structure of these chemicals is presented in Fig. 1. Filipin is a mixture of four macrolides with minor differences in their structures (Bergy and Eble, 1968), the fraction known as filipin III being the major component.

The experimental procedure to obtain small unilamellar vesicles (SUV) was previously described (Castanho and Prieto, 1992); filipin was incorporated from injections of stock solutions in buffer in the present work. In experiments with MLV, incorporation of quenchers was carried out using

Received for publication 28 November 1994 and in final form 4 April 1995.
Address reprint requests to Dr. Manuel Jose Estevez Prieto, Centro Quimica Fisica Molecular, Instituto Superior Tecnico, Av. Rovisco Pais, 1096 Lisboa Codex, Portugal. Tel.: 351-1-841929; Fax: 351-1-3524372. E-mail: qmprieto@alfa.ist.utl.pt

0006-3495/95/07/155/14 $2.00

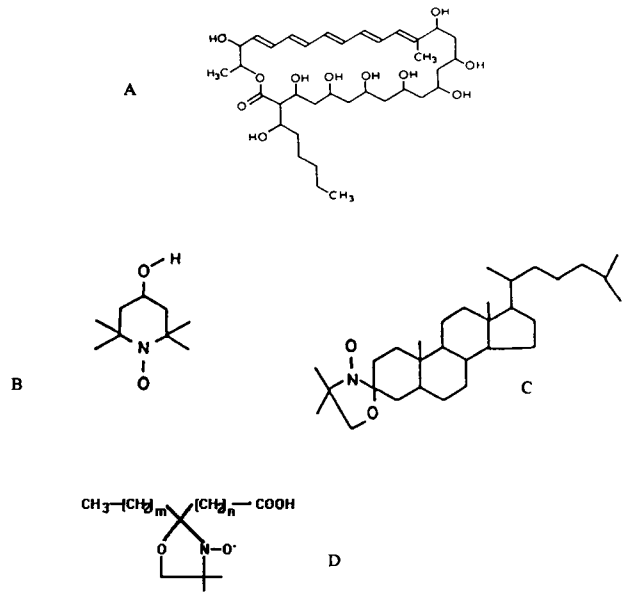

FIGURE 1 Molecular structure of (*A*) filipin III; (*B*) TEMPOL; (*C*) 3NC; (*D*) 5NS: n = 3, m = 12°d 16NS: n = 14, m = 1.

the co-solubilization method, i.e., they were added to a chloroform solution of the lipid, before proceeding with the usual method to obtain the MLV. The lipid (or lipid/quencher mixture) was suspended directly in a filipin solution. Hence, the antibiotic can equilibrate in all lamellae.

The partition constant, K_p, of filipin into the MLV (results not shown) was determined from the variation of antibiotic anisotropy upon increasing lipid concentration, as described elsewhere (Castanho and Prieto, 1992). Values of $K_p = (5.0 \pm 1.0) \times 10^3$ and anisotropy in the lipid, $r_l = 0.29 \pm 0.01$ were obtained from a nonlinear regression fit, assuming the molar volume of the lipid to be $\gamma_l = 0.83$ dm^3/mol (calculated from x-ray data described in Davenport et al., 1985; gel phase). As the partition constant in MLV is higher than the one reported for SUV ($K_p = (3.4 \pm 0.8) \times 10^3$; Castanho and Prieto, 1992), the first lipidic system was chosen for the quenching experiments. On the other hand the curvature effects in SUV could also be a limiting factor in the sterol incorporation in the membrane above ≈20% (molar) of sterol (results not shown).

The contribution to the total fluorescence intensity by filipin present in the aqueous phase could bias the application of a Stern-Volmer formalism of quenching for filipin incorporated in the membrane (when using lipophilic probes). This possible problem was carefully considered. Given the calculated K_p value, we conclude that for the lipid concentrations used (3.5 mM), the fraction of incorporated filipin is 95%. Since the total filipin concentration is 10^{-5} M the concentration remaining in the aqueous phase is 5.10^{-7} M; Hence, this fraction of filipin is essentially monomeric (Castanho et al., 1994) and due to its low intrinsic quantum yield (ϕ_w = 0.08; Castanho et al., 1992) contributes only 1.5% of the total fluorescence observed. Using the method described in Appendix I, it can be concluded that the Stern-Volmer ratios of fluorescence intensity are affected less than 10%. It should be stressed that identical experimental conditions were also described by other authors (Atik and Singer, 1978; Bieri and Walach, 1975b).

Corrections for the effective quencher concentrations in the membrane are also needed, as these probes also partition between the two phases. This problem is addressed in Appendix I. All the possible artifacts present in steady state fluorescence intensity measurements were considered. Namely, the geometry factor is insignificant for the concentrations used, and the inner filter effect (fluorescence reabsorption) and the excitation light partition between fluorophore and quencher were accounted for in the data processing as described elsewhere (Coutinho and Prieto, 1993). The critical radius of energy transfer R_o, was evaluated from a rewritten Förster formula as previously described (Berberan-Santos and Prieto, 1987). Unless otherwise stated, all the experiments were carried out at 25°C in 5 mm rectangular cuvettes, with excitation and emission wavelengths of 338 and 480 nm, respectively, in steady state experiments. The 337 nm nitrogen line was used for excitation in time-resolved experiments.

THEORETICAL BACKGROUND

Transient effects in dynamic fluorescence quenching were studied by Nemzek and Ware (1975). These authors demonstrated that the fluorescence decay in the presence of quencher in 3D (unit efficiency of collision, $\gamma = 1$) is described by:

$$I(t) = I(0) \cdot \exp\left[-\frac{t}{\tau_0} - 4\pi R D N_A [Q] t \left(1 + \frac{2R}{\sqrt{\pi D t}}\right)\right] \quad (1)$$

where: τ_0 = fluorescence lifetime, R = collisional radius, D = mutual diffusion coefficient of fluorophore and quencher, N_A = Avogadro's number, and Q = molar concentration of the quencher. This leads to the Stern-Volmer steady state relationship:

$$\frac{I_{f,0}}{I_f} = (1 + 4\pi R D \tau_0 N_A [Q]) Y^{-1} \quad (2)$$

$$Y = 1 - \frac{\beta}{\sqrt{\alpha}} \sqrt{\pi}\, e^{\beta^2/\alpha}\, \mathrm{erfc}\left(\frac{\beta}{\sqrt{\alpha}}\right) \quad (3)$$

$$\alpha = \frac{1}{\tau_0} + 4\pi R D N_A [Q] \quad (4)$$

$$\beta = 4R^2 \sqrt{\pi D N_A [Q]} \quad (5)$$

where I_f and $I_{f,0}$ are the fluorescence intensities at $[Q]$ and $[Q] = 0$, respectively, and erfc is the complementary error function.

The fluorophores in biochemical heterogeneous systems usually present intrinsic complex fluorescence decays, even in the absence of quencher, and the application of the above formalism to experimental data is not feasible. However, fast transient components are usually not too important. The fluorescence decay is, in most cases, described by a single exponential function for each subpopulation with specific photophysical properties (e.g., solvation effects, polarity, excited state reactions). The transient effects are not considered in detail. The total decay is then described by a sum of exponential functions (Eq. 6).

$$I(t) = \sum_i a_{0,i} \cdot e^{-t/\tau_{0,i}} \quad (6)$$

Simpler models can then be applied to each component of the total decay, namely the ones describing static effects. These effects would reduce the preexponential factors ($a_{0,i}$), which are proportional to the concentrations of excited species at the instant of excitation, while the dynamic quenching decreases the lifetimes, $\tau_{0,i}$. When considering the probability that fluorophore and quencher in a random distribution are in contact at the instant of excitation

(quenching sphere of action; Perrin, 1927), Eqs. 7 and 8 are obtained (Castanho and Prieto, 1992):

$$I(t) = \sum_i a_{0,i} \cdot e^{-t/\tau_i} \quad (7)$$

$$\frac{I_{f,o}}{I_f} = \frac{\sum_i (a_{0,i}\,\tau_{0,i})}{\sum_i (a_{0,i} e^{-VN_A\,\gamma[Q]\tau_i})} \quad (8)$$

where τ_i is the fluorescence lifetime at $[Q]$, γ is the quenching efficiency, and V_i is the volume surrounding the fluorophore, where the quencher has to be located, so that quenching occurs instantaneously with probability γ.

If the associations between fluorophore and quencher are not random and can be described by a 1:1 association constant, K_A (ground state complex model; Lakowicz, 1983):

$$K_A = \frac{[FQ]}{[F][Q]} \quad (9)$$

(F = fluorophore; Q = quencher), Eqs. 10 and 11 are derived (Appendix II):

$$I(t) = \sum_i \frac{a_{0,i}}{1 + K_A[Q]_i} \cdot e^{-t/\tau} \quad (10)$$

$$\frac{I_{f,o}}{I_f} = \frac{\sum_i (a_{0,i}\tau_{0,i})}{\sum_i \left(\frac{a_{0,i}}{1 + K_A[Q]_i}\,\tau_i\right)} \quad (11)$$

It is interesting to note that the sphere of action model is the limit of the ground state complex model for a very weak association ($K_A \to 0$; if $x \approx 0$ then $e^x \approx 1 + x$).

Eqs. 7 and 10 are simple to use in a global data analysis when fitting fluorescence transient state experimental data. Assuming a unique K_A or V for all the fluorophore subpopulations, the number of fitting parameters is decreased in systems with more than two subpopulations of fluorophores. It should be stressed that V and γ can be obtained from experiments in homogeneous medium (aqueous solutions, in the present study) and compared with theoretical expectations (see next section). The estimation of diffusion coefficients from the Stokes-Einstein equation (Lakowicz, 1983), and the encounter radii from the addition of atomic volumes (Edward, 1970), allows the efficiency parameter for the molecular reaction, γ, to be obtained.

According to the model assumptions, its validity implies that the following should be observed:

1) Linear Stern-Volmer plots in transient state ($\tau_{0,i}/\tau_i$ versus $[Q]$). From the slope, the bimolecular rate constant for quenching, k_q, is obtained (Eq. 12, Smoluchowski equation; Lakowicz, 1983):

$$k_q = \gamma 4\pi N_A R_{PQ} D_{PQ} \quad (12)$$

where R_{PQ} is the collisional radius (taken as the sum of the Van der Waals radii of fluorophore and quencher), and D_{PQ} is the sum of their diffusion coefficients.

2) V is the volume of the sphere that surrounds the fluorophore with radius R, which should be close to the sum of the molecular radii of F and Q, for contact interactions.

3) Eqs. 8 and 11 should enable the recovery of the Stern-Volmer plot obtained in steady state conditions.

Equations similar to Eqs. 8 and 11 were obtained by Laws and Contino (1992); however, the quencher efficiency, both in transient and static quenching (Castanho and Prieto, 1992), was not accounted for in their treatment.

RESULTS

Filipin fluorescence quenching by TEMPOL in aqueous phase

Upon mixing filipin (13 μM) and TEMPOL (0.44 M) in aqueous solution, a new absorption band is observed centered at 725 nm, with a low molar absorption coefficient ($\epsilon = 4 \times 10^2\ M^{-1}\ cm^{-1}$) (result not shown). In addition filipin fluorescence is efficiently quenched; in Fig. 2 are shown the Stern-Volmer plots for filipin monomer quenching (0.6 μM), and for the aggregate quenching (30 μM). The aggre-

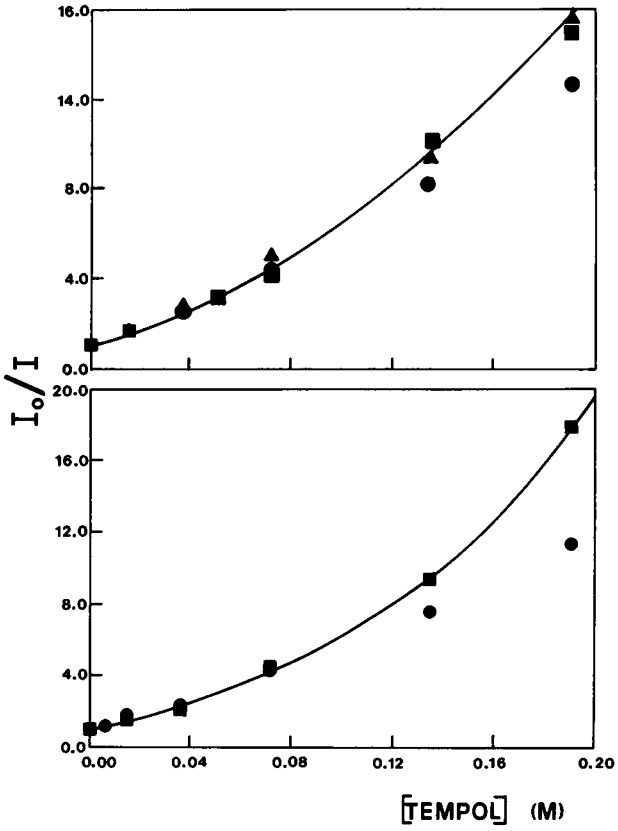

FIGURE 2 Steady state Stern-Volmer plot (■) for the fluorescence quenching of filipin monomer (A; 0.6 μM) and aggregate (B; 30 μM) by TEMPOL in water. Recovered Stern-Volmer plot from transient state data according to Eq. 11 (▲ complexation model $K_a = 3\ M^{-1}$) and Eq. 8 (●, sphere of action model; $\gamma = 0.5$, $R = 1.0$ nm)

gation behavior in aqueous solution of this antibiotic was previously studied (Castanho and Prieto, 1992; Castanho et al., 1993).

The upward curvature of the Stern-Volmer plots points to the existence of a static quenching mechanism. To further elucidate this question, Stern-Volmer plots in transient state were obtained, both for the monomer and the aggregate (results not shown). The monomer decay is monoexponential with a lifetime $\tau = 14$ ns (Castanho and Prieto, 1992); an expected linear Stern-Volmer relationship was obtained, a bimolecular quenching rate constant $k_q = 2.8.10^9\ M^{-1}\ s^{-1}$ being determined, implying a value $\gamma = 0.5$ (Eq. 12). The aggregate has a complex decay, which can be described by three components ($a_1 = 0.39$, $\tau_1 = 15.1$ ns; $a_2 = 0.26$, $\tau_2 = 6.6$ ns; $a_3 = 0.35$, $\tau_3 = 1.5$ ns; Castanho and Prieto, 1992). The bimolecular quenching rate constants obtained for each component are very similar, $k_q = 2.2 \times 10^9\ M^{-1}\ s^{-1}$ (longer component), $k_q = 3.7 \times 10^9\ M^{-1}\ s^{-1}$ (intermediate component), and $k_q = 3.0 \times 10^9\ M^{-1}\ s^{-1}$ (shorter component). The steady state Stern-Volmer plot can be recovered with $V = 4.2\ nm^3$ in Eq. 8.

Filipin fluorescence decay in membranes

The filipin fluorescence decay in the gel phase of MLV of DPPC (22°C) is complex, being described by three components ($a_1 = 0.06$, $\tau_1 = 33.4$ ns; $a_2 = 0.20$, $\tau_2 = 17.4$ ns; $a_3 = 0.74$, $\tau_3 = 1.0$ ns). This last component is eventually biased by light scatter because of the large vesicle volume; in agreement, with SUV of DPPC (20°C) only two components are required ($a_1 = 0.6$, $\tau_1 = 22.6$ ns; $a_2 = 0.4$, $\tau_2 = 11.1$ ns; Castanho and Prieto, 1992). In this way, only the first two ones were considered in transient data analysis. In Fig. 3 is presented the variation of filipin lifetime upon increase in temperature both in buffer (the shorter component is omitted) and incorporated in SUV of DPPC. A linear variation is obtained in homogeneous solution, and this photophysical parameter is clearly sensitive to the phase transition of the lipid. No lifetime variation was observed upon increase of antibiotic in the membrane in the concentration range of 0.1–50 μM.

Filipin fluorescence quenching by lipophilic probes

The steady state Stern-Volmer plots for filipin fluorescence quenching by the lipophilic probes 5NS, 16NS, and 3NC are shown in Fig. 4. In all cases the variations are nonlinear, with a downward curvature; the more efficient quencher is 3NC, and 5NS is the least efficient one.

Detailed experimental data will be presented separately for each quencher.

Quenching by 5NS

When the transient state data (results not shown) are treated according to the sphere of action model (Eq. 7) with the same parameters previously obtained from the monomer quenching study in aqueous phase ($V = 4.2\ nm^3$, $\gamma = 0.5$), linear Stern-Volmer relationships in transient state were obtained; the bimolecular rate constants obtained are $k_q = 8.9.10^7\ M^{-1}\ s^{-1}$ (short lifetime component), and $k_q = 2.6.10^7\ M^{-1}\ s^{-1}$ (long lifetime component). In addition, it is possible to recover the steady state plot (Eq. 8) as shown in Fig. 5 *A*.

Quenching by 16NS

The sphere of action model, (Eqs. 7 and 8) cannot describe the quenching kinetics by this species when the previous parameters ($V = 4.2\ nm^3$, $\gamma = 0.5$) are used; as shown in Fig. 5 *B*, from the lifetime data, an underestimated steady state quenching plot is obtained, unless unreasonably high values of both γ and V are used. Moreover, the transient state Stern-Volmer plot obtained is nonlinear for the shorter lifetime component. From the ground state complex model (Eq. 11; $K_A = 3\ M^{-1}$), it is possible to recover the steady

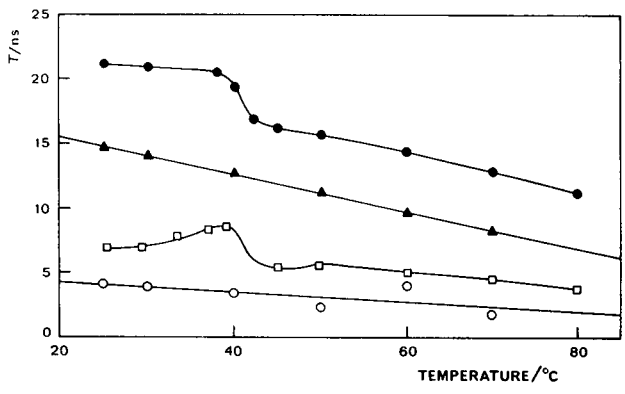

FIGURE 3 Filipin fluorescence lifetime components versus temperature in aqueous solution (▲,○), and in the presence of SUV of DPPC (●,■). (Fit to two components in both cases).

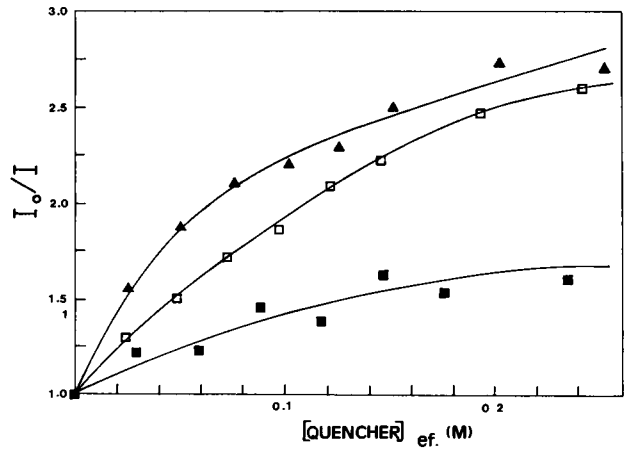

FIGURE 4 Steady state Stern-Volmer plot for the fluorescence quenching of filipin incorporated in MLV of DPPC by the lipophilic quenchers 3NC (▲), 16NS (□), and 5NS (■).

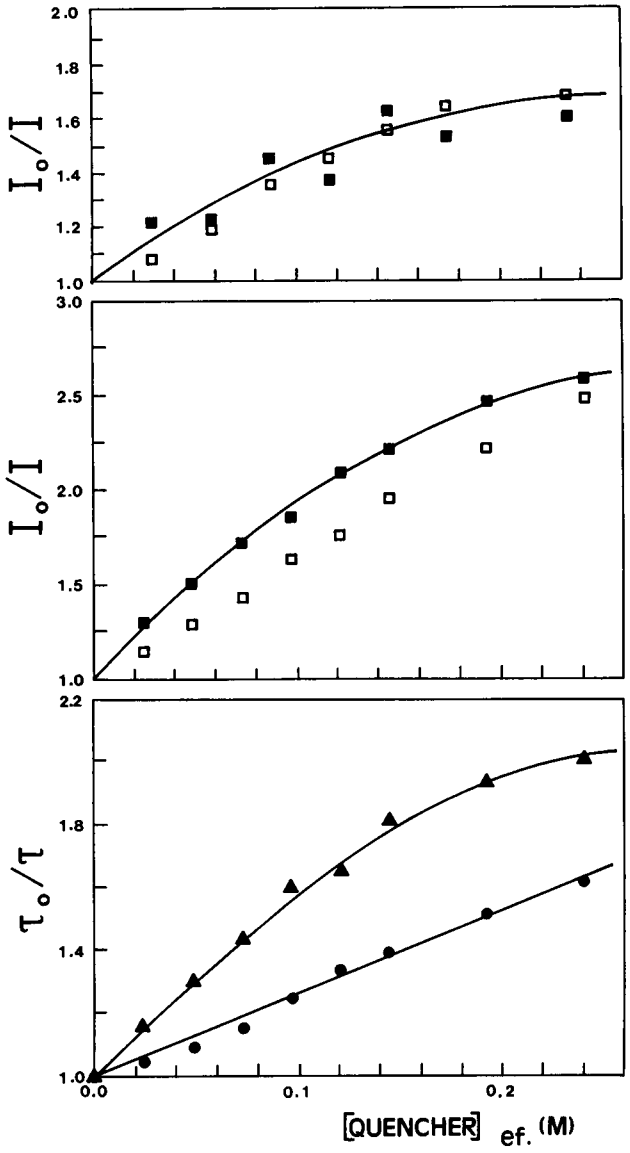

FIGURE 5 Steady state (*A* and *B*) and transient (*C*), Stern-Volmer plots for the fluorescence quenching of filipin in MLV of DPPC by (*A*) 5NS (■, experimental; □, from Eq. 8, $V = 4.2$ nm^3, $\gamma = 0.5$), (*B*) 16NS (■, experimental; □, from Eq. 8, $V = 4.2$ nm^3, $\gamma = 0.5$), (*C*) 16NS (▲, short lifetime component; ●, long lifetime component), Eq. 11 ($K_A = 3$ M^{-1}).

state Stern-Volmer plot, but again a nonlinear relationship is obtained for the shorter lifetime component, as shown in Fig. 5 *C*. The bimolecular quenching rate constants are $k_q = 7.6 \times 10^7$ M^{-1} s^{-1} (long lifetime component), and $k_q = 38.9 \times 10^7$ M^{-1} s^{-1} (short lifetime component), this last one obtained from the initial slope of the plot.

Quenching by 3NC

When this cholesterol spin probe is used as a quencher, a steady state quenching plot is obtained with an inflection ~50 mM. When trying to apply the sphere of action model with the same parametrization used for the other probes, linear transient state quenching plots are obtained (results not shown), but it is not possible to correctly reproduce the steady state Stern-Volmer plot (Eq. 8) as shown in Fig. 7. There is also no fit with the complexation model (Eq. 11) as depicted in the same figure; with an association constant $K_A = 20$ M^{-1}, the initial regime is described, but at higher concentrations there is a large deviation with an upward curvature.

DISCUSSION

Filipin fluorescence quenching by TEMPOL in aqueous phase

The mechanism of quenching

As shown below (in Kinetics of Quenching), TEMPOL is very effective as a quencher of filipin fluorescence with an efficiency $\gamma = 0.5$ and a collisional radius of quenching $R = 1.0$ nm. The new band observed on the filipin absorption spectrum ($\lambda = 725$ nm) upon the presence of TEMPOL is attributed to the $T_1 \leftarrow S_0$ transition of the polyene; in agreement the T_1 energy reported for a pentaene (Evans, 1960) corresponds to a wavelength $\lambda = 729$ nm. This fact clearly demonstrates that TEMPOL induces spin-orbital coupling on the polyene leading to an increased intersystem crossing. The low value of $\epsilon = 4 \times 10^2$ M^{-1} cm^{-1} is compatible with the forbidden character of the transition.

Recently Matko et al. (1992), following the work of Green et al. (1990), presented a detailed study on the mechanism of quenching of aromatic molecules by paramagnetic species. From their work it can be concluded that the contribution of energy transfer mechanisms either dipolar (Förster, 1959) or exchange (Dexter, 1953) is negligible, the dominant mechanism being the electron exchange orbital mixing. In our system the contribution of Förster type energy transfer can also be ruled out; we obtained for the filipin monomer-TEMPOL pair a critical radius of transfer $R_o = 1.0$ nm, a similar value being obtained when the donor is the aggregate. These small values rule out the applicability of the Förster theory since the donor and the acceptor can no longer be described as point dipoles.

The determined efficiency of filipin quenching by TEMPOL ($\gamma = 0.5$) is one order of magnitude higher than the one obtained with iodide ($\gamma = 0.05$; Castanho and Prieto, 1992). The heavy-atom effect of iodide, due to spin-orbital coupling via a charge transfer mechanism, is inefficient with the pentaene, as was also observed for the polyenes retinol and retinal (Song et al., 1976). The iodide absorption is at much higher energy than the filipin fluorescence preventing electron exchange; on the contrary the antibiotic emission overlaps with the first absorption band of the paramagnetic species (centered at a wavelength $\lambda = 430$ nm; $\epsilon = 14$ M^{-1} cm^{-1} in agreement with Green et al., 1990) The small oscillator strength of this absorption renders a dipolar energy transfer negligible as previously discussed, but the Dexter type of energy transfer is not ruled out on this basis for our system. In addition, this process is not forbidden for a doublet-state acceptor (Razi-Naqvi,

1981). However, this mechanism is certainly not the most important, considering the existence of spin-orbital coupling as shown from the induced $T_1 \leftarrow S_0$ absorption of the antibiotic.

Another argument in favor of the spin-orbital coupling via exchange mechanism stems from the value recovered for the radius of interaction $R = 1.0$ nm (see Theoretical Background section), slightly higher than the sum of the molecular radius of fluorophore and quencher ($\approx$0.7 nm as determined from Edward's procedure (Edward, 1979)). This observation is characteristic of exchange interactions as found by others (Martinho, 1989). The interaction distances range from 0.5 to 2 nm (Matko et al., 1992), a value of 1.2 nm being reported by Green et al. (1990).

Kinetics of quenching

Following the procedure described in the Theoretical Background section, it is concluded that the process is nearly diffusion-controlled ($\gamma = 0.5$). Considering this high value of γ, the importance of a static contribution for the quenching, as shown by the upward curvature of the Stern-Volmer relationships in Fig. 2, is not surprising. In agreement with the iodide quenching of filipin, where $\gamma = 0.05$ is one order of magnitude smaller, no deviation from linearity was observed (Castanho and Prieto, 1992).

The monomer steady state quenching Stern-Volmer plot can be adequately recovered according to both models as shown in Fig. 2 *A*), a deviation being observed for the sphere of action model for the higher quencher concentrations. The best fit to Eq. 8 was obtained with $V = 4.2$ nm^3, while from the complexation model (Eq. 11) $K_A = 3$ M^{-1} was found. The sphere volume corresponds to a radius of 1.0 nm, this value being slightly higher than the sum of molecular radii as discussed previously. The value of $K_A = 3$ M^{-1} would correspond to a very weak interaction. In this limit the fraction of associated fluorophore and quencher would be identical to the one obtained from the statistical distribution of molecules. In this way, while a weak complexation cannot be ruled out for the higher quencher concentrations ($[Q] > 0.1$ M), the quenching mechanism is essentially dynamic.

The filipin aggregate steady state quenching can be rationalized with the same model parameters used for the monomer as shown in Fig. 2 *B*; in this case independent quenching of the three components of the complex decay is considered. In addition, the identical quenching efficiency observed for the differents components is in favor of an open structure of the aggregate regarding the TEMPOL molecule. This was also previously concluded from a quenching study with iodide ion (Castanho and Prieto, 1992). As previously described, the global agreement between monomer and aggregate decay rationalization further supports the sphere of action model. After the analysis of the photophysical interaction in homogeneous medium, we can now proceed with the study in membranes. Before that, the multiexponential filipin fluorescence decay in vesicles will be revisited, as this information is essential to the eventual topological conclusions.

Filipin fluorescence decay in membranes

As with other polyenes, namely the tetraene parinaric acid (Sklar et al., 1977), filipin is able to monitor the phase transition of DPPC (Fig. 3), a decrease in both lifetime components being observed. However, the variation of quantum yield is much smaller than the one observed with the tetraene. This experiment was carried out to compare the two chromophores. Before proceeding with the fluorescence quenching study a brief comment on the nature of the lifetime components is relevant.

The photophysics of parinaric acid in heterogeneous media has been a matter of debate (Sklar et al., 1977; Wolber and Hudson, 1981; Parasassi et al., 1984; James et al., 1987; Ruggiero and Hudson 1989; Mateo et al., 1993), but the following conclusions seem supported by clear experimental evidence. 1) Although the tetraene has a complex decay even in homogeneous media, the longer lifetime component in membranes can be safely assigned to the probe in a gel phase. This is concluded from the higher anisotropy values associated with this component as well as from a red shift in the excitation spectrum. 2) The persistence of this component (with a small amplitude), above the gel-to-liquid crystal phase transition (T_c) in lipidic membranes, is due to the existence of structural fluctuations of the membrane, which span a time longer than the fluorescence lifetime of the probe. 3) The shorter lifetime component observed at temperatures below T_c is due to probe-induced local perturbations in the membrane. 4) Lifetime distributions can certainly be used to describe the fluorescence decay, but the result is essentially identical to the one obtained with discrete components.

The very low filipin solubility in non-aqueous solvents prevents the realization of a detailed photophysical study. For the interpretation of the quenching data in membranes, the same situation as applicable to parinaric acid will be considered, i.e., the shorter and longer components reflect probe populations in the "liquid crystal"-like (more disordered) and "gel"-like (more ordered) phases, respectively. In this way, it is not surprising to observe fluorescence dynamic quenching in a lipidic system below T_c. Labeled fatty acids are not immobile in gel phase membranes (Hauser et al., 1979; Derzko and Jacobson, 1980). Moreover, Derzko and Jacobson (1980) calculated diffusion coefficients of several kinds of probes in DMPC using fluorescence recovery after photobleaching techniques and always detected two diffusive components. The slower component ($D \approx 10^{-11}$ cm^2 s^{-1}) is attributed to diffusion in highly ordered areas of the membrane, while the faster component (10^{-10} cm^2 s$^{-1} < D < 10^{-8}$ cm^2 s^{-1}) is related to the several kinds of defects that are present in the gel phase. It is interesting to note that the slow diffusional component of an NBD (7-nitrobenz-2-oxa-1,3-diazole-4-

yl)-labeled fatty acid is still higher than the average. These values are $D \approx 10^{-9}$ cm^2 s^{-1} (slow component) and $D \approx 10^{-8}$ cm^2 s^{-1} (fast component). Such results and interpretations have been reported by others; e.g., Balcom and Peterson (1993) studied the diffusion of impurities in bilayers and suggested a distribution of the molecules between the gel matrix and the defects.

The observed invariation of filipin lifetime, upon its concentration in the membrane, rules out the existence of any significant dynamic self-quenching, at variance with results observed with parinaric acid (Morgan et al., 1980).

Filipin fluorescence quenching by lipophilic probes

As described in the Theoretical Background section, diffusion in membranes was considered to take place in an isotropic 3D medium. If the membrane was strictly bidimensional, different boundary conditions for the Smoluchowski formalism should be applied (Razi-Naqvi, 1974). The best approach to the specific situation of probe diffusion in a membrane is the one used by Owen (1975), in which the finite bilayer width is considered (cylindrical geometry). Owen (1975) introduced the parameter τ_s, which defines the transition from the spherical (3D) to the cylindrical geometry, its value being $\tau_s = 42$ ns when considering the bilayer and the filipin parametrization. This value is longer than the lifetime of filipin, so the 3D consideration is essentially correct. Almgren (1991), in a comparative study of quenching in restricted dimensionality, states that deviations from 3D occur only for very long fluorescence lifetimes.

Quenching by 5NS

As described in the Results section, the sphere of action model rationalizes all the data as the two following criteria are verified. 1) Linear Stern-Volmer relationships are obtained in transient state, and 2) the steady state plot is correctly recovered from the lifetime data (Fig. 5 *A*). This reasoning implies that 5NS is essentially randomly distributed in the membrane. Hauser et al. (1979) using electron spin resonance (ESR) and electrophoretic mobility measurements, showed that there is no significant aggregation of 5NS, in concentrations up to 10% mol (however, liquid crystal membranes were used). The bimolecular quenching rate constant for the short lifetime component is slightly higher than the longer lifetime component. This would be compatible with the following arguments. 1. The long lifetime corresponds to probes in the gel phase (Ruggiero and Hudson, 1989), which would have smaller diffusion coefficients, and 2) the quencher partition between the two phases favors the liquid crystal domain (Butler et al., 1974). In this way its effective concentration would be greater, and an apparently higher rate constant is observed). As shown, a dynamic mechanism of quenching is observed for both lifetime components, which points to a significant diffusion of the molecular species. As previously described, in a gel phase membrane these areas are the structural defects limiting the highly ordered regions where diffusion is negligible. It can then be concluded that filipin is segregated to these areas, which can also be induced by the probe itself.

Quenching by 16NS

For this quencher, both the complexation and the sphere of action model are unable to rationalize the experimental data. The downward curvature of the transient state Stern-Volmer plot can only be understood if the diffusion coefficient D and/or the effective quencher concentration are decreasing with the increase in total quencher concentration. Both these arguments are compatible with an aggregation of the 16NS probes. There is no detailed independent information to formulate a precise model to describe the quencher aggregation. However, postulating simple assumptions regarding the type and size of the aggregates, it is possible to demonstrate that a nonlinear transient state plot is expected.

Assuming that the quencher molecules are forming aggregates with a Gaussian distribution of sizes, Eq. 13 is derived (Appendix III),

$$\frac{\tau_0}{\tau} = 1 + \tau_0 [Q]_m \frac{\sum_{N=1}^{\infty} (K_{q,N} e^{-A})}{\sum_{N=1}^{\infty} (N \cdot e^{-A})} \qquad (13)$$

where

$$A = \frac{(N - N_m)^2}{2\sigma^2} \qquad (14)$$

where N and N_m are the aggregation number and the mean aggregation number respectively, $[Q]_m$ is the molar concentration, σ the distribution standard deviation and $K_{q,N}$ is the bimolecular quenching rate constant for the aggregate of N molecules. This value is obtained from the Smoluschowski equation (Eq. 12), taking into account the corrected value for the diffusion coefficient of the aggregate.

For the dependence of N_m on $[Q]_m$, a simple linear variation is considered (Eq. 15),

$$N_m = N_{m,o} + INT(K'[Q]_m) \qquad (15)$$

where $N_{m,o}$ is the minimum allowed aggregation ($N_{m,o} = 1$) and K' is a constant.

In Fig. 6 are shown the theoretical expected variations of τ_0/τ (further details can be found in Appendix III). Nonlinear plots are obtained upon the increase of K (Fig. 6 *A*), while the major effect of σ is the variation of the slope of the plot (Fig. 6 *B*). Certainly, with some aggregation models other than the Gaussian, an identical conclusion would be expected, i.e., nonlinear transient plots would be obtained. It should be stressed that the derived model is not a demonstration that 16NS aggregates in membranes according to a

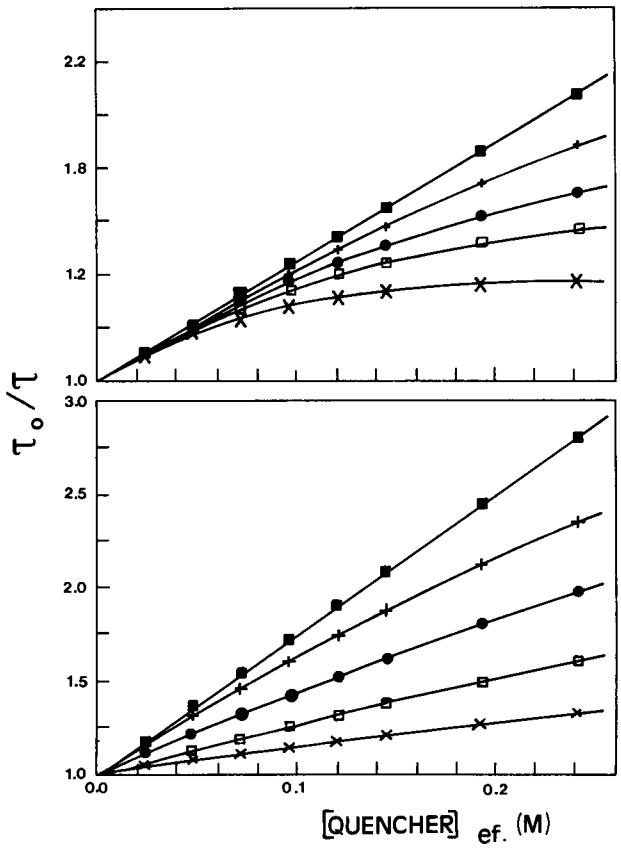

FIGURE 6 Theoretical transient state Stern-Volmer plot (Eqs. 14 and 15; details in Appendix III) assuming quencher aggregation. (*A*) $K' = 1$, ■; $K' = 2$, +; $K' = 4$, ●; $K' = 6$, □; $K' = 10$, ×; (*B*) $\sigma = 0.1$, ■; $\sigma = 0.5$, +; $\sigma = 1$, ●; $\sigma = 2$, □; $\sigma = 4$, ×)

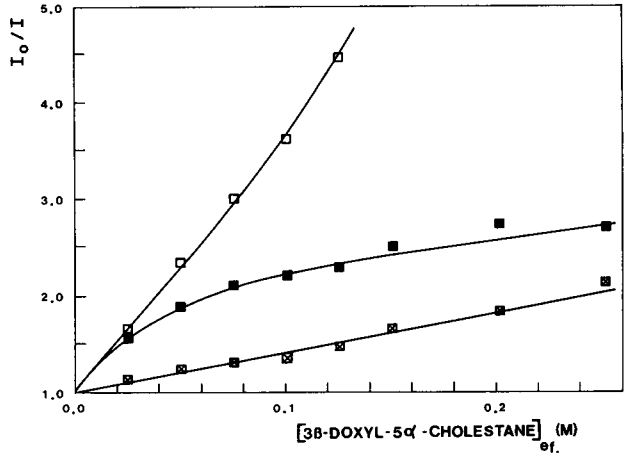

FIGURE 7 Steady state Stern-Volmer plot for the fluorescence quenching of filipin in MLV of DPPC by 3NC (■). Theoretical variation from Eq. 8 ($V = 4.2$ nm^3, $\gamma = 0.5$; ⊠), and Eq. 11 ($K_A = 20$ M^{-1}; □).

Gaussian size distribution; rather it provides evidence that aggregation in fact occurs. This is supported by the work of Hauser et al. (1979), who demonstrated that the onset for the aggregation of this probe is very low (≈5% molar) (although this result is reported in a liquid-crystal phase membrane).

Quenching by 3NC

For the sterol spin probe, a more pronounced inflection in the quenching plot was obtained as shown in Fig. 7. The sphere of action model, which assumes a random distribution of both fluorophore and quenchers, cannot describe the experimentally observed fluorescence quenching. The same result is obtained with the complexation model, which in any case cannot explain a downward curvature. It was previously shown for the 16NS probe that a downward curvature could be rationalized by a model assuming probe aggregation; however, biphasic type behavior is not expected for any gradual aggregation process. We propose that this behavior is due to phase separation, i.e., an extreme situation of aggregation, in which sterol-rich domains are formed. The observed inflection point corresponds to a 3% molar fraction of sterol, this value being close to the one where the DPPC/cholesterol phase diagram in the gel phase shows the formation of sterol domains in the membrane (Vist and Davis, 1990). Below this concentration, there is a nearly random distribution of cholesterol, to which filipin is weakly associated ($K_A = 20$ M^{-1}). This weak association is further supported by the results of Maurin et al. (1988), who studied the association of 25-doxyl-27-norcholesterol with filipin via ESR, and also by the ^{2}H-nuclear magnetic resonance results of Dufourc and Smith (1985), where it is apparent that cholesterol prevents the direct interaction of the antibiotic with the lipids.

Further conclusions regarding the antibiotic organization in the membrane can be inferred from the present study. The spin probe used as a quencher is identical to a cholesterol in which the hydroxyl group is substituted by a polar moiety, the nitroxide label. Hence the 3NC molecules should have a similar location to cholesterol in the membrane, i.e., parallel to the lipids and included in the palisade structure. The weak interactions observed do not seem effective enough to induce an alteration of this location, contrary to the model of De Kruijff and Demel (1974), in which long and planar aggregates of filipin and sterol in between the two layers are postulated. The results of the present work are in agreement with Dufourc and Smith (1985), and do not contradict the hypothesis of Elias et al. (1979).

Filipin location in DPPC bilayers

Fluorescence quenching by labeled fatty acids at different chain positions has been used to obtain information on probe location in membranes (Bieri and Wallach, 1975a,b; Wardlaw et al., 1987). This methodology is based on several assumptions, namely identical diffusion coefficients and intrinsic efficiencies, γ, for the distinct quenchers used. In this scheme, the different modes of fluorescence quenching obtained (either static or dynamic), are due to different local concentrations of the quencher in the fluorophore vicinity.

Once the quencher position is assessed by an independent method, the probe location may be inferred.

In our work we assumed that the intrinsic quenching efficiency, γ, is identical for all quenchers, this being the value in aqueous solution, i.e., there is no specific stereochemical or polarity dependence. The short and long lifetime components of filipin decay were assigned to subpopulations in the liquid crystal and gel phases, respectively (Ruggiero and Hudson, 1989); as the diffusion coefficients of the 5NS and 16NS probes are identical, the values of k_q relative to each component can be intercompared. The values obtained in both phases are larger for the 16NS probe (k_q^{5NS} (short component) = $8.9 \times 10^7\ M^{-1}\ s^{-1}$; k_q^{5NS} (long component) = $2.6 \times 10^7\ M^{-1}\ s^{-1}$; K_q^{16NS} (short component) = $38.9 \times 10^7\ M^{-1}\ s^{-1}$; K_q^{16NS} (long component) = $7.6 \times 10^7\ M^{-1}\ s^{-1}$). Hence, we can conclude that both filipin subpopulations are located away from the membrane interface, near the 16NS probe. In addition, the experimental bimolecular rate constant is greater for the subpopulation in the "liquid crystal phase," as expected (greater D), this result being obtained for both quenchers. However, this conclusion cannot be immediately reached, as the partition constant of the fatty acid probes favors (i.e., greater Q) the liquid crystal phase (Butler et al., 1974), and a similar behavior could happen in the present case.

A different methodology to locate filipin (the parallax model) can be applied to our steady state data (Chattopadhyay and London, 1987). In this approach it is assumed a static and random distribution of fluorophore and quenchers, i.e., an active-sphere model, is the only operating quenching mechanism. Although these considerations do not apply to our systems, as there is experimental evidence for variation of probe lifetime (dynamic contribution), its application for the sake of comparison points to a conclusion similar to the one obtained with our model. The location obtained is 2.1 nm away from the interface, near the 10^{th} carbon of the fatty acid chain, i.e., in between carbons 5 and 16. A recent refinement of the parallax model (Abrams and London, 1992) accounts for transverse motion of quenchers relative to fluorophores, where the closest approach of F and Q is considered shorter (on average). In this way, an apparent (and greater) quenching sphere of action is obtained, which includes the dynamic quenching contribution. Application of this refined model further supports our conclusion (location of the fluorophore closer to the center of the bilayer). Considering vertical displacements of 0.2–0.4 nm in the quencher position during excited state lifetime, similar uncertainties in the fluorophore location are obtained. It should be stressed that, according to the refined parallax method theory of Abrams and London (1992), if lateral and transverse components of motion occur and are equal (i.e., the motion is close to isotropic) then their effects on apparent fluorophore depth cancel out.

The results obtained with the 3NC quencher cannot be directly compared with the other probes. This probe does not belong to the fatty acid series of quenchers, and in addition its mechanism is essentially static. However, it is reasonable to assume that, in agreement with another report (Ohki et al., 1979), its specific interaction with filipin displaces the antibiotic to the surface where the sterol is located. Membrane structural alterations are observed in microscopy upon the presence of sterol (Tillack and Kinsky, 1973; Verkleig et al., 1973), these being due to the described displacement to the interface. In sterol-free membranes, the antibiotic is located inside the membrane as concluded from this work, and in this way microscopic alterations are not apparent. It should be stressed that we demonstrated recently that filipin incorporates into the membranes even in the absence of sterol (Castanho and Prieto, 1992).

CONCLUSION

A detailed photophysical study of the fluorescence quenching of the antibiotic filipin by spin probes was carried out with the aim of determining its transverse location in a model system of membranes. In addition, information regarding fatty acids organization in membranes was also obtained. The formalism used is based on the analysis of transient state quenching data of the complex decay (2 or 3 exponentials). A linear relationship should be obtained for each case, and from the variation of lifetimes (dynamic) and amplitudes (static), the steady state plot should be correctly recovered. Both sphere of action and complexation models of quenching were used.

From a study in aqueous solution it was concluded that the nitroxide has a near unit ($\gamma = 0.5$) quenching efficiency, its mechanism being the induced spin-orbital coupling (as concluded from $T_1 \leftarrow S_0$ absorption), eventually via electron exchange. Both transient and steady state quenching plots are rationalized upon a sphere of action model of quenching. The quenching sphere of action model also holds for the 5NS quencher (consequently, we can conclude that this probe is essentially randomly distributed in the membrane). At variance with this conclusion, no agreement was obtained for either the complexation or the sphere of action model with 16NS, nonlinear downward quenching plots being obtained. This observation is compatible with probe aggregation. When using a cholesterol-derivative 3NC, a biphasic behavior was observed, which was rationalized assuming phase separation above 3% molar of cholesterol. Higher bimolecular quenching rate constants were obtained for 16NS as compared with 5NS. From these results, we conclude that filipin, in the absence of cholesterol, is located deep inside the membrane. A distance of 2.1 nm from the interface is obtained, based only on static quenching.

The antibiotic action of filipin

Considering our present and previous results (Castanho et al., 1992, 1994; Castanho and Prieto, 1992), and data published by others, we propose that the fundamental aspects

that control the biochemical action of filipin are 1) the concentration of sterol present in the membrane (more precisely, if it is organized in domains or not); and 2) the total concentration of filipin (depending on the value of the partition constant, K_p, filipin in the water phase may be monomeric or aggregated). As we shall describe, an increasing intensity of effects can be detected upon the increase of sterol and/or antibiotic concentration. So, for the sake of clarity, we will consider separately two ranges of sterol concentration, corresponding to two different organizations in the membranes (one with sterol randomly distributed and other with sterol-forming domains).

Low concentration of sterol

Using electronic microscopy techniques, Maurin et al. (1988) and Tillack and Kinsky (1973) failed to detect any filipin effect in egg yolk lecithin membranes, below a limit of 5 and 10% (molar), respectively. Clejan and Bittman (1985) detected a breakpoint at ~4% (molar) of several sterols in the binding rate of amphotericin B. In the present work, a biphasic type behavior was detected, with a transition at 3%. These values are very close to the ones in which phase transition is detected in pure lipid/cholesterol phase diagrams (e.g., Vist and Davis, 1990; Almeida et al., 1992).

In this low range of concentrations filipin associates with sterols. Backes and Rychnovsky (1992) using high performance liquid chromatography techniques determined K_A = 42 M^{-1} for the filipin-3NC association, which is in agreement with the value K_A = 20 M^{-1} obtained in the present study. However, these authors have also used other sterols, reaching higher values (280 M^{-1}, epiandrosterone; 700 M^{-1}, ergosterol; 1.4 × 10^4 M^{-1}, cholesterol). These small aggregates (assumed to be dimers) of filipin/sterol can be parallel to the plane of the bilayer (Flick and Gelerinter, 1977; 1% sterol). Ohki et al. (1979) proposed that these small aggregates could self-associate upon temperature decrease.

Maurin et al. (1988) observed that, to have leakage of encapsulated compounds when the sterol concentration is low, a higher concentration of filipin had to be used. In this case, a similar effect to that produced by Triton X-100 can be obtained. We assign this action to the presence of filipin aggregates (Castanho and Prieto, 1992; Castanho et al., 1994) in the aqueous medium surrounding the membranes, i.e., filipin (an amphipathic molecule) acts on the membrane as a detergent. The interaction between filipin and sterol-free membranes has been proposed earlier (Milhaud et al., 1989; Castanho and Prieto, 1992; Milhaud, 1992). As concluded in the present work, in this case filipin is buried in the center of the bilayer. According to Milhaud (1992) filipin is segregated in membrane domains without specifying its transverse location.

High concentration of sterol

Maurin et al. (1988) demonstrated the existence of two filipin subpopulations in membranes with a high concentration of sterols. One of these subpopulations is free filipin, while the other is bound to sterols. If the filipin:cholesterol ratio is >30, all the sterol is bound to filipin and separated from the phospholipids. This would explain why phase transition in membranes containing sterols and filipin can be similar to the one in pure lipids (Norman et al., 1972). Dufourc and Smith (1985), concluded that filipin/sterol domains are still located in the lipid bilayer matrix; however, at higher filipin concentrations there might be an exclusion of these mixed aggregates from the surface of the bilayer. This would explain the results obtained by Elias et al. (1979) and the "holey sheets" observed by Behnke et al. (1984); while the mixed aggregates are in the lipid matrix, they lay on the surface of the bilayer (Ohki et al., 1979). This explains why the filipin effect can only be detected by microscopy if sterols are present in high concentrations.

It should be emphasized that the antibiotic-induced perturbation becomes more intense upon increasing the antibiotic concentration. We propose that, as long as the sterol is segregated in domains, filipin interacts preferentially with these domains disordering the membranes. If the antibiotic concentration is increased the sterol domains might saturate, which means that filipin then has to interact with the pure phospholipid and K_p decreases (results not shown). As a consequence, there is a tendency for filipin aggregation in the aqueous medium. When filipin self-aggregates (Castanho et al., 1994), it may act as a detergent, extracting sterol from the lipidic matrix.

APPENDIX I

Stern-Volmer relationship for a fluorophore that partitions between the membrane and the aqueous phase

In the case where both fluorophore (F) and quencher (Q) partition between the lipidic (l) and aqueous (w) phases (the partition constants being $K_{P,F} = [F]_l/[F]_w$ and $K_{P,Q} = [Q]_l/[Q]_w$) two different Stern-Volmer relationships are obtained (Eqs. AI.1 and AI.2) in which the variables have the usual meaning:

$$I_{f,w} = \frac{I_{0,w}}{1 + K_{SV,w}[Q]_w} \quad \text{(AI.1)}$$

$$I_{f,l} = \frac{I_{0,l}}{1 + K_{SV,l}[Q]_l} \quad \text{(AI.2)}$$

Then the total light emitted, $I_{f,t}$, relative to the case in the absence of quencher $I_{0,T}$, is obtained summing up the two contributions:

$$\frac{I_{0,t}}{I_{f,t}} = \frac{(1 + K_{SV,w}[Q]_w)(1 + K_{SV,l}[Q]_l)(I_{0,w} + I_{0,l})}{I_{0,w}(1 + K_{SV,l}[Q]_l) + I_{0,l}(1 + K_{SV,w}[Q]_w)} \quad \text{(AI.3)}$$

In the case where the fluorophore partition in the membrane was total ($K_{P,F} = \infty$), Eq. AI.4 would hold,

$$\frac{I_{0,T}}{I_{f,T}} = 1 + K_{SV,l}[Q]_l \qquad \text{(AI.4)}$$

Then, for a quencher concentration $[Q]$, the following ratio between the experimental intensities is defined, considering the existence of fluorophore partition:

$$\frac{\left(\frac{I_{0,T}}{I_{f,T}}\right)_{K_{P,F}\in R}}{\left(\frac{I_{0,T}}{I_{f,T}}\right)_{K_{P,F}=\infty}} = \frac{1 + K_{SV,W}[Q]_W}{\eta'(1 + K_{SV,I}K_{PQ}[Q]_W) + (1 - \eta')(1 + K_{SV,W}[Q]_W)} \qquad \text{(AI.5)}$$

where $\eta' = I_{o,w}/I_{o,t}$.

The effective quencher concentration in the membrane $[Q]_l$ is determined from the total quencher concentration $[Q]_T$ via a correction factor C_f,

$$[Q]_l = [Q]_T \cdot C_f \qquad \text{(AI.6)}$$

which is derived as

$$C_f = \left(1 - \frac{K_{P,Q}\gamma_l[L]}{1 - \gamma_l[L] + K_{P,Q}\gamma_l[L]}\right)\frac{K_{P,Q}}{1 - \gamma_l[L]} \qquad \text{(AI.7)}$$

where γ_l is the lipid molar volume, and $[L]$ the lipid molar concentration. The first factor of this equation is the quencher molar concentration in the aqueous phase. The parameter ($K_{q,l}$ and $K_{P,Q}$) values for the nitroxide quenchers used were taken from the literature (Wardlaw et al., 1987). For the lipid $\gamma_l = 0.873\ dm^3\ mol^{-1}$ was considered (calculated from x-ray data described in Davenport et al., 1985). In Fig. 8, Eq. AI.5 is represented. As the experimental conditions correspond to $\eta' \approx 0.015$ and $[Q]_l \leq 0.25$ M, it can be concluded that the expected maximum deviation of the Stern-Volmer relationship is 10%, which enables the application of the photophysical models used, namely, Eqs. 8 and 11.

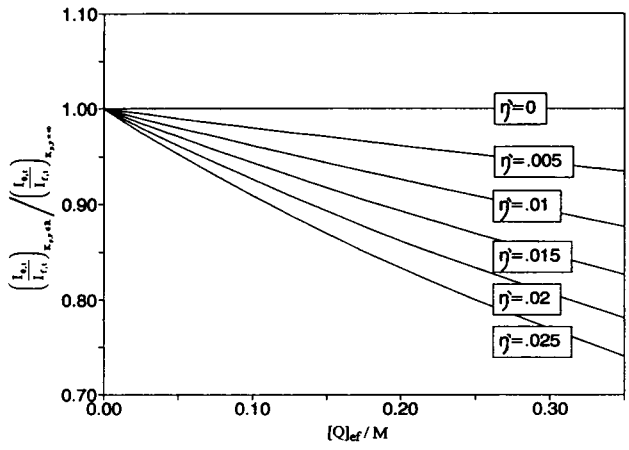

FIGURE 8 Ratios of the Stern-Volmer relationship (Eq. AI.5) (consideration of fluorophore partition between lipidic and aqueous phases) versus quencher concentration in the membrane for various η' values, assuming $[F]_T = 10$ mM and $[L] = 3.5$ mM.

APPENDIX II

Static mechanism of quenching by complexation

In the case where the fluorophore has a complex decay,

$$I(t) = \sum_i a_i e^{-t/\tau_i} \qquad \text{(AII.1)}$$

where τ_i is the lifetime component, and a_i the preexponential factor. When the fluorophore and quencher associate, the equilibrium constant K_A is defined as:

$$K_A = \frac{[FQ]}{[F][Q]} \qquad \text{(AII.2)}$$

where $[FQ]$ is the concentration of non-fluorescent complex (static quenching). The preexponential factor is solely proportional to the concentration of free fluorophore existing in equilibrium conditions ($a\ \alpha[F]$), which is given by

$$[F] = \frac{[F]_t}{1 + K_a[Q]_t} \qquad \text{(AII.3)}$$

once that $[Q] \approx Q]_t$ is assumed (i.e., low K_a value). In this way,

$$a_i\alpha\frac{[F_t]}{1 + K_a[Q]_t} \qquad \text{(AII.4)}$$

and

$$a = \frac{a_0}{1 + K_a[Q]_t} \qquad \text{(AII.5)}$$

where a_o and a are the preexponential factors in the absence and in the presence of a quencher concentration $[Q]$.

The following decay law is then

$$I(t) = \sum_i \left(\frac{a_{0,1}}{1 + K_A[Q]_t} e^{-t/\tau_i}\right) \qquad \text{(AII.6)}$$

When describing the steady state intensity from the integrated decay law,

$$I = \int_0^\infty I(t)dt \qquad \text{(AII.7)}$$

the following relationship is obtained.

$$\frac{I_{f,0}}{I_f} = \frac{\sum_i (a_{0,i}\tau_{0,i})}{\sum_i \left(\frac{a_{0,i}\tau_{0,i}}{1 + k_A[Q]_t}\tau_i\right)} \qquad \text{(AII.8)}$$

APPENDIX III

Transient state Stern-Volmer relationship assuming quencher aggregation with a Gaussian distribution of sizes

Assuming that N molecules of quencher are forming disk-type aggregates in the membrane, its diffusion is equivalent to the sphere with the same radius, $R_{Q,N}$. The dependence of $R_{Q,N}$ on the aggregation number N is obtained, considering that the quencher molecules are organized in an hexagonal lattice:

$$R_{Q,N} = d \cdot \log_2\left(\frac{N+5}{6}\right) \qquad \text{(AIII.1)}$$

where d is the radius increase upon covering one more layer of the hexagonal lattice. The bimolecular quenching rate constant $k_q(N)$, can also be obtained from the Smoluschowski equation:

$$k_q(N) = \gamma 4\pi N_A R_{P,Q}(D_P + D_{Q,N}(N)) \qquad \text{(AIII.2)}$$

where the variables have the same meaning as described in Eq. 12.

For the derivation of a Stern-Vomer relationship, it is still necessary to evaluate the concentration of the aggregate species $[Q_N]$. For this purpose, a Gaussian distribution for the $[Q_N] = f(N)$ function was assumed:

$$\frac{[Q_N]}{[Q_{N_m}]} = \exp\left(-\frac{(N - N_m)^2}{2\sigma^2}\right), \qquad \text{(AIII.3)}$$

N_m and σ being the distribution parameters. The total quencher concentration, $[Q]_m$, is then

$$[Q]_m = \sum_{N=1}^{\infty}(N[Q_m]) \qquad \text{(AIII.4)}$$

The Stern-Volmer relationship considering the effect of the quencher aggregation is:

$$\frac{\tau_0}{\tau} = 1 + \tau_0[Q]_m \frac{\sum_{N=1}^{\infty}(K_{q,N}e^A)}{\sum_{N=1}^{\infty}(N \cdot e^{-A})}; \qquad \text{(AIII.5)}$$

$$A = \frac{(N - N_m)^2}{2\sigma^2}$$

It should be stressed that this expression can be reformulated as:

$$\frac{\tau_0}{\tau} = 1 + \tau_0\langle k_{q,N}\rangle\langle[Q]_m\rangle \qquad \text{(AIII.6)}$$

where $\langle K_{q,N}\rangle$ and $\langle[Q]_m\rangle$ are the average values over the aggregation number N.

The preexponential factor a should also be reduced as described in Eq. 7, because of the static contribution (sphere of action of quenching)

$$a \,\alpha\, [F]_m\, e^{-N_A\gamma\sum_{N=1}^{\infty}(V_N[Q_N])}, \qquad \text{(AIII.7)}$$

V_N being the volume of the aggregate of N molecules, which can be described as a cylindrical shell with internal and external radius $R_{Q,N}$ and $(R_{Q,N} + R_{PQ})$ respectively, and height R_{PQ}.

From Eq. AIII.3 and AIII.7, then, one obtains

$$\frac{a}{a_0} = \exp(-N_A\gamma\pi R_{PQ}^2[Q]f(N_m)) \qquad \text{(AIII.8)}$$

where $f(N_m)$ is

$$f(N_m) = \frac{\sum_{N=1}^{\infty}[(2R_{Q,N} + R_{P,Q})e^{-A}]}{\sum_{N=1}^{\infty}(N \cdot e^{-A})}; \qquad \text{(AIII.9)}$$

$$A = \frac{(N - N_m)^2}{2\sigma^2}$$

Finally it is necessary to know the dependence of N_m on $[Q]_m$. In the absence of detailed physical information, a simple linear relationship was assumed:

$$N_m = N_{m,o} + INT(K'[Q]_m) \qquad \text{(AIII.10)}$$

where K' is a constant, and $N_{m,o} = 1$ is the minimum allowed aggregation number.

The transient state Stern-Volmer plot obtained on the assumptions of this model was presented in Fig. 6. The value $d = 0.8$ nm was taken, corresponding to the area of a phospholipid headgroup (Davenport et al., 1985); $R_{PQ} = 1$ nm and $\gamma = 0.5$ were determined from experiment.

The authors gratefully acknowledge Dr. A. U. Acuña (Consejo Superior de Investigaciones Cientificas, Madrid, Spain) for the helpful discussion of the results.

This work was supported by Junta Nacional de Investigação Científica e Tecnológica (Portugal), programs STRDA/C/SAU/257/92 and STRDA/C/CEN/421/92.

REFERENCES

Abrams, F. S., and E. London. 1992. Calibration of the parallax fluorescence quenching method for determination of membrane penetration depth: refinement and comparison of quenching by spin-labeled and brominated lipids. *Biochemistry*. 31:5312–5322.

Almeida, P. F. F., W. L. C. Vaz, and T. E. Thompson. 1992. Lateral diffusion in the liquid phases of dimyristoylphosphatidylcholine/cholesterol lipid bilayers: a free volume analysis. *Biochemistry*. 31: 6739–6747.

Almgren, M. 1991. Kinetics of excited state processes in micellar media. *In* Kinetics and Catalysis in Microheterogeneous Systems. M. Gratzel, and K. Kalyanasundaram, editors. Marcel Dekker, New York. 63–113.

Atik, S. S., and L. A. Singer. 1978. Nitroxyl radical quenching of the pyrene fluorescence in micellar environments. Development of a kinetic model for steady-state and transient experiments. *Chem. Phys. Lett.* 59:519–524.

Backes, B. J., and S. D. Rychnovsky. 1992. A reverse-phase HPLC assay for measuring the interaction of polyene macrolide antifungal agents with sterols. *Anal. Biochem.* 205:96–99.

Balcom, B. J., and N. O. Petersen. 1993. Lateral diffusion in model membranes is independent of the size of the hydrophobic region of molecules. *Biophys. J.* 65:630–637.

Behnke, O., J. Tranurn-Jensen, and B. V. Deurs. 1984. Filipin as a cholesterol probe. 1. Morphology of filipin-cholesterol interaction in lipid model systems. *Eur. J. Cell. Biol.* 3:189–199.

Berberan-Santos, M. N., and M. J. E. Prieto. 1987. Energy transfer in spherical geometry. Application to micelles. *J Chem. Soc. Faraday Trans. II.* 83:1391–1409.

Bergy, M., and T. Eble. 1968. The filipin complex. *Biochemistry.* 7: 653–659.

Bieri, V. G., and D. F. M. Wallach. 1975a. Variations of lipid-protein interactions in erythrocyte ghosts as a function of temperature and pH in physiological and non-physiological ranges. *Biochim. Biophys. Acta.* 406:415–423.

Bieri, V. G., and D. F. M. Wallach. 1975b. Fluorescence quenching in lecithin and lecithin/cholesterol liposomes by paramagnetic lipid analogues. Introduction of a new probe approach. *Biochim. Biophys. Acta.* 389:413–427.

Bolard, J. 1986. How do polyene macrolide antibiotics affect the cellular membrane properties?. *Biochim. Biophys. Acta.* 864:257–304.

Butler, K. W., N. M. Tattrie, and C. P. Smith. 1974. The location of spin probes in two phase mixed lipid systems. *Biochim. Biophys. Acta.* 363:351–360.

Castanho, M. A. R. B., and M. Prieto. 1992. Fluorescence study of the macrolide pentaene antibiotic filipin in aqueous solution and in a model system of membranes. *Eur. J. Biochem.* 207:125–134.

Castanho, M. A. R. B., A. Coutinho, and M. Prieto. 1992. Absorption and fluorescence spectra of polyene antibiotics in the presence of cholesterol. *J. Biol. Chem.* 267:204–209.

Castanho, M. A. R. B., W. Brown, and M. Prieto. 1994. Filipin and its interaction with cholesterol in aqueous media studied using static and dynamic light scattering. *Biopolymers.* 34:447–456.

Chattopadhyay, A., and E. London. 1987. Parallax method for direct measurement of membrane penetration depth utilising fluorescence quenching by spin-labeled phospholipids. *Biochemistry.* 26:39–45.

Clejan, S., and R. Bittman. 1985. Rates of amphotericin B association with sterols. *J. Biol. Chem.* 260:2884–2889.

Coutinho, A. and M. Prieto. 1993. Ribonuclease T1 and alcohol dehydrogenase fluorescence quenching by acrilamide. *J. Chem. Educ.* 70: 425–428.

Davenport, L., R. E. Dale, R. M. Bisby, and R. B. Cundall. 1985. Transverse location of the fluorescent probe 1,6-diphenyl-1,3,5-hexatriene in model lipid bilayer membrane systems by resonance excitation energy transfer. *Biochemistry.* 24:4097–4108.

De Kruijff, B., and R. A. Demel. 1974. Polyene-sterol interactions in membranes of *Acholeplasma laidlawii* cells and lecithin membranes. III. Molecular structure of the polyene antibiotic-cholesterol complexes. *Biochim. Biophys. Acta.* 339:57–70.

Derzko, Z., and K. Jacobson. 1980. Comparative lateral diffusion of fluorescent lipid analogues in phospholipid multilayers. *Biochemistry.* 19:6050–6057.

Dexter, D.L. 1953. A theory of sensitised luminescence in solids. *J. Chem. Phys.* 21:836–850.

Dufourc, E. J., and C. P. Smith. 1985. ^{2}H-NMR evidence for antibiotic-induced cholesterol immobilisation in biological membranes. *Biochemistry.* 24:2420–2424.

Edward, J. T. 1970. Molecular volumes and the Stokes-Einstein equation. *J. Chem. Educ.* 47:261–70.

Elias, P. M., D. S. Friend, and J. Goerke. 1979. Membrane sterol heterogeneity. Freeze-fracture detection with saponins and filipin. *J. Histochem. Cytochem.* 27:1247–1260.

Evans, D. F. 1960. Magnetic perturbation of singlet-triplet transitions. Part IV. Unsaturated compounds. *J. Chem. Soc.* 1960:1735–1745.

Flick, C., and E. Gelerinter. 1977. Cholestane spin label study of filipin action on lipid planar multibilayers. *Chem. Phys. Lipids.* 18:62–72.

Forster, T. 1959. Transfer mechanisms of electronic excitation. *Disc. Faraday Soc.* 27:7–17.

Green, S. A., D. J. Simpson, G. Zhou, P. S. Ho, and N. V. Blough. 1990. Intramolecular quenching of excited singlet states by stable nitroxyl radicals. *J. Am. Chem. Soc.* 112:7337–7346.

Hauser, M., W. Guyer, and K. Howell. 1979. Lateral distribution of negatively charged lipids in lecithin membranes. Clustering of fatty acids. *Biochemistry.* 18:3285–3291.

James, D. R., J. R. Turnbull, B. D. Wagner, W. R. Ware, and N. O. Petersen. 1987. Distributions of fluorescence decay times for parinaric acids in phospholipid membranes. *Biochemistry.* 26:6272–6277.

Kinsky, S. C., S. A. Luse, and L. L. M. Van Deenen. 1966. Interaction of polyene antibiotics with natural and artificial membrane systems. *Fed. Proc.* 25:1503–1510.

Lakowicz, J. R. 1983. Principles of Fluorescence Spectroscopy. Plenum Press, New York. 257–275.

Laws, W. R., and P. B. Contino. 1992. Fluorescence quenching studies: analysis of nonlinear Stern-Volmer data. *Methods Enzymol.* 210: 448–463.

Martinho, J. M. G. 1989. Heavy-atom quenching of monomer and excimer pyrene fluorescence. *J. Phys. Chem.* 93:6687–6692.

Mateo, C. R., J.-C. Brochon, M. P. Lillo, and U. Acuña. 1993. Lipid clustering in bilayers detected by the fluorescence kinetics and anisotropy of trans-parinaric acid. *Biophys. J.* 65:2248–2260.

Matko, J., K. Ohki, and M. Edidin. 1992. Luminescence quenching by nitroxide spin labels in aqueous solution: studies on the mechanism of quenching. *Biochemistry.* 31:703–711.

Maurin, L., F. Banchl, P. Morin, and A. Bienvenue. 1988. Interactions between a paramagnetic analogue of cholesterol and filipin. *Biochim. Biophys. Acta.* 939:102–110.

Milhaud, J. 1992. Permeabilizing action of filipin III on model membranes through a filipin-phospholipid binding. *Biochim. Biophys. Acta.* 1105: 307–318.

Milhaud J., J. Mazerski, J. Bolard, and E. J. Dufourc. 1989. Interaction of filipin with dimyristoylphosphatidylcholine membranes studied by ^{2}H-NMR, circular dichroism, electronic absorption and fluorescence. *Eur. Biophys. J.* 17:151–158.

Morgan, C. G., B. Hudson, and P. K. Wolber. 1980. Photochemical dimerization of parinaric acid in lipid bilayers. *Proc. Natl. Acad. Sci. USA.* 77:26–30.

Nemzek, T. L., and W. R. Ware. 1975. Kinetics of diffusion controlled reactions: transient effects in fluorescence quenching. *J. Chem. Phys.* 62:477–489.

Norman, A. W., R. A. Demel, B. De Kruijff, and L. L. M. Van Deenen. 1972. Studies on the biological properties of polyene antibiotics. Evidence for the direct interaction of filipin with cholesterol. *J. Biol. Chem.* 247:1918–1929.

Ohki, K., Y. Nozawa, and S. 1. Ohnishi. 1979. Interaction of polyene antibiotics with sterols in phosphatidylcholine bilayer membranes as studied by spin probes. *Biochim. Biophys. Acta.* 554:39–50.

Owen, C. S. 1975. Two dimensional diffusion theory: cylindrical diffusion model applied to fluorescence quenching. *J. Chem Phys.* 62:3204–3207.

Parasassi, T., F. Conti, and E. Gratton. 1984. Study of heterogeneous emission of parinaric acid isomers using multifrequency phase fluorometry. *Biochemistry.* 23:5660–5670.

Perrin, J. 1927. Fluorescence and molecular induction by resonance. *Comp. Rend. Acad. Sci. Paris.* 184:1097–1100

Razi-Naqvi, K. 1974. Diffusion-controlled reactions in two dimensional fluids: discussion of measurements of lateral diffusion of lipids in biological membranes. *Chem. Phys. Lett.* 28:280–284.

Razi-Naqvi, K. 1981. Spin selection rules concerning intermolecular energy transfer. Comments on "Energy-transfer studies using doublet-state acceptors." *J. Phys. Chem.* 85:2303–2304.

Ruggiero, A., and B. Hudson. 1989. Critical density fluctuations in lipid bilayers detected by fluorescence lifetime heterogeneity. *Biophys. J.* 55:1111–1125.

Severs, N. J., and H. Roebenek. 1983. Detection of microdomains in biomembranes. An appraisal of recent developments in freeze-fracture cytochemistry. *Biochim. Biophys. Acta.* 737:373–408.

Sklar, A., B. S. Hudson, and R. D. Simoni. 1977. Conjugated polyene fatty acids as membrane probes: synthetic phospholipid membrane studies. *Biochemistry.* 16:819–828.

Song, P. S., Q. Chae, M. Fuijta, and B. Hiroaki. 1976. Electronic relaxation processes in retinol and retinal: anomalous external heavy-atom effect

and temperature dependence of fluorescence. *J. Am. Chem. Soc.* 98: 819–824.

Tillack, T. W., and S. C. Kinsky. 1973. A freeze-etch study of the effects of filipin on liposomes and erythrocytes membranes. *Biochim. Biophys. Acta.* 323:43–54.

Verkleij, A. J., B. De Kruijff, W. F. Gerritsen, R. A. Demel, L. L. M. Van Deenen, and P. H. J. Ververgaert. 1973. Freeze-etch electron microscopy of erythrocytes, *Acholeplasma laidlawii* cells and liposomal membranes after the action of filipin and amphotericin B. *Biochim. Biophys. Acta.* 291:577–581.

Vist, M. R., and J. M. Davis. 1990. Phase equilibria of cholesterol/dipalmitoylphosphatidylcholine mixtures: ^{2}H nuclear magnetic resonance and differential scanning calorimetry. *Biochemistry.* 29:451–464.

Wardlaw, J. R., W. H. Sawyer, and K. P. Ghiggino. 1987. Vertical fluctuation of phospholipid acyl chains in bilayers. *FEBS Lett.* 231: 20–24.

Wolber, P. K., and B. S. Hudson. 1981. Fluorescence lifetime and time-resolved polarisation anisotropy studies of acyl chain order and dynamics in lipid bilayers. *Biochemistry.* 20:2800–2810.